Optical-absorption studies of ion-implantation damage in Si on sapphire

U. Zammit, K. N. Madhusoodanan, M. Marinelli, F. Scudieri, R. Pizzoferrato, and F. Mercuri
Dipartimento di Ingegneria Meccanica, II Università di Roma "Tor Vergata," Via della Ricerca Scientifica, 00173 Rome, Italy

E. Wendler and W. Wesch
Institut für Festkörperphysik, Friedrich-Schiller-Universität Jena, Max-Wien-Platz 1, D-07743 Jena, Germany
(Received 17 November 1993)

A detailed study of the implantation-induced damage in Si on sapphire, carried out by optical-absorption measurements extending from energies above the band gap down to energies far into the subgap region of Si, is presented. The changes induced in the optical band gap, band-edge slopes, and in the subgap features of the spectra are carefully described. The various stages of formation and quenching of divacancies were monitored as a function of implantation conditions and annealing cycles through their 1.8-μm absorption band. It is shown that the divacancies strongly affect the population of band-tail states and the annealing studies revealed that the progressive quenching of the divacancy band is followed by the appearance of another absorption band, characteristic of some intrinsic secondary defect, whose annealing behavior is similar to the one observed for the five-vacancy electron-paramagnetic-resonance spectrum. The study of the structural relaxation process in implanted a-Si gave indications that the process is indeed associated with annihilation of defects as well as average strain reduction in the material, in agreement with earlier indications. Finally, some common features, such as band-edge inverse-logarithmic slope values and subgap features, are found in annealed implanted crystalline and a-Si.

INTRODUCTION

Radiation damage in Si has been studied for the past 30 years. Its interest nowadays is mainly directed toward the understanding and application of the damage accumulated during ion implantation of the material because of its technological implications for device fabrication and, recently, for "defect engineering." While in the former case the damage must be removed in order to achieve adequate electrical activation of the implanted atoms and of carrier mobility, the latter procedure refers to the controlled introduction of ion-induced damage to achieve the desired properties of the material.[1–4] This is obtained by engineering the interactions between the induced defects and implanted atoms through a suitable choice of the implantation conditions and annealing cycles and therefore derives from a thorough knowledge of damage nucleation and evolution during implantation and subsequent annealing cycles.

In its amorphous structure, implanted Si has very recently drawn considerable attention because of the mechanisms inducing changes in its physical properties upon annealing, referred to as "structural relaxation." Amorphous Si (a-Si) is generally viewed as a continuous random network of tetrahedrally coordinated covalently bonded atoms.[5] Upon annealing, the positions of all the atoms in the network evolve, giving rise to variations of the average network parameters, such as reduction of the tetrahedral bond-angle distortion and therefore of the average strain in the material. Great attention has been devoted to structural relaxation in ion-implanted a-Si since there have been indications that this process occurs through annihilation of defects of the same kind as the ones observed in damaged crystalline material.[6] Point defects like vacancies and vacancy-impurity complexes have in fact been detected in ion-implanted a-Si.[7]

The study of the different aspects of radiation damage in Si involved a great variety of techniques, amongst which electron paramagnetic resonance (EPR) is certainly of major importance, since it has provided that microscopic information at the atomic level which has led to the identification of several defects in irradiated Si. Amongst the intrinsic ones, such defects include the divacancy,[8] the four-vacancy[9] and the five-vacancy[10] complexes, and the di-interstitial.[11] EPR has also enabled the determination of the absolute concentration of the observed defects. Subgap absorption has also proved useful in studying irradiation-induced defects in Si. Absorption bands at 1.8, 3.3, and 3.9 μm have been associated with the various charge states of the divacancy, the most prominent intrinsic defect stable at room temperature.[12,13] Moreover, for the known divacancy concentration determined by EPR and the absorption measured at the 1.8-μm band, it was possible to correlate the magnitude of the absorption against the divacancy concentration.[13] This has enabled one to monitor the concentration of divacancies in ion-implanted Si by subgap absorption as a function of both the implantation conditions and the annealing cycles.[14] Monitoring of defects by subgap absorption is, in fact, with respect to EPR, less subject to indetermination due to changes in the charge states of the defects which may be induced during processing of the material and which can turn the defect from paramagnetic to diamagnetic.[15]

Investigations of the various aspects of structural relaxation of implanted a-Si also involved a variety of tech-

niques including calorimetry,[6] electrical measurements,[16,17] metal diffusion,[6,18] and Raman spectroscopy.[6] Even in the case of amorphous material, however, optical absorption can prove useful since, besides being sensitive to defects in the subgap region, in the region at and above the band edge, both the band-edge inverse-logarithmic slope and the optical band gap depend on the average disorder or strain in the material as observed in hydrogenated *a*-Si (*a*-Si:H).[19] Optical-absorption measurements can therefore provide a complete picture of the processes occurring during structural relaxation of ion-implanted *a*-Si.

In this paper we present a detailed study of the implantation-induced damage in Si by optical-absorption measurements extending from energies above the band gap down to energies far into the subgap region of Si, in order to obtain further information on the investigated phenomena. The changes induced in the optical band gap, band-edge slopes, and in the subgap features of the spectra are carefully described. The various stages of formation and quenching of divacancies were monitored as a function of implantation conditions and annealing cycles. It is shown that the divacancies strongly affect the population of band-tail states. Studies carried out in annealed damaged crystalline material reveal that the progressive annealing of the divacancy band is followed by the appearance of another absorption band, characteristic of some intrinsic secondary defect, whose annealing behavior is similar to the one observed for the five-vacancy EPR spectrum. Finally, the study of the structural relaxation process in implanted *a*-Si gives indications that the process is indeed associated with annihilation of defects as well as average strain reduction in the material.

EXPERIMENT

The investigations were performed on 800-nm-thick [100] intrinsic Si on sapphire (SOS) layers in order to be able to measure absorption even in the spectral region above the band gap. The optical-absorption measurements were performed by photothermal deflection spectroscopy (PDS),[20,21] a highly sensitive technique, which allows detection of low levels of absorption, typical of the subgap region of semiconductors, even in layers as thin as the ion-implanted ones. This has enabled us to obtain absorption data starting from 2.6–2.8 eV and extending down to 0.48 eV, an energy far into the subgap region of Si. The low-energy limitation in our setup was merely due to the absorption by our refractive optics and PDS cell window. With a suitable choice of optics we thus plan to have access to lower energies in the near future. The interference vs energy oscillation effect in the PDS spectra was eliminated by determining the ratio of the simultaneously determined transmission to the PDS spectra, as suggested for photoconductivity measurements.[22] An oscillation-free resulting spectrum is obtained in this way. Moreover, the resulting spectrum does not depend on eventual wavelength-dependent reflectivity variations that can occur over the investigated spectral region. Absolute absorption values were obtained by normalizing the spectra with respect to corresponding values obtained in the spectral region where the samples were optically opaque.

The implantation was carried out at 80 and 300 K and, on each sample, ions were implanted at 150 and 300 keV (dose ratio 0.4:1) in order to obtain a fairly uniform, relatively thick ($\sim$500 nm) implanted layer. Self-ion irradiation was chosen to eliminate the effects arising from chemically dissimilar ions on the damage formation and evolution. The damage profile in the samples were determined by Rutherford backscattering (RBS, not shown) and the structure of the implanted layers was monitored by reflection high-energy electron diffraction (RHEED, not shown).

RESULTS AND DISCUSSION

A. Effect of implantation conditions

Figures 1(a) and 1(b) show the spectra relative to the samples implanted with increasing ion dose (dose values refer to the total dose implanted in each sample) at 300 K, while Fig. 2 refers to the corresponding results for 80-K implantation. The lower absorption observed for the higher implantation temperature reflects the effect of the partial annealing of the damage which occurs during 300-K implantation. It should be remarked that the layer implanted at 80 K with a dose of 8.4×10^{14} cm^{-2} consisted of a uniform amorphous layer, while the other implantations led to the formation of nonuniform damaged layers consisting of damaged crystalline material or of a mixture of amorphous and damaged crystalline material.

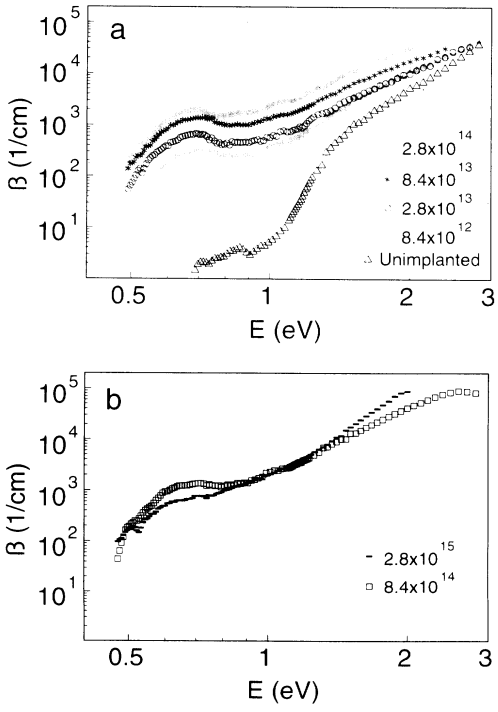

FIG. 1. (a), (b) Dose dependence of the absorption spectra of room-temperature-implanted Si on sapphire (SOS) films. (a) refers to doses in cm^{-2}.

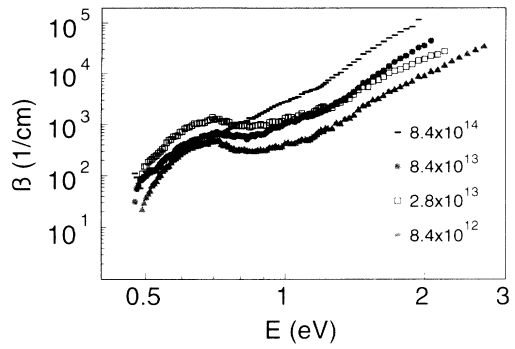

FIG. 2. Dose dependence of the absorption spectra of 80-K-implanted SOS films.

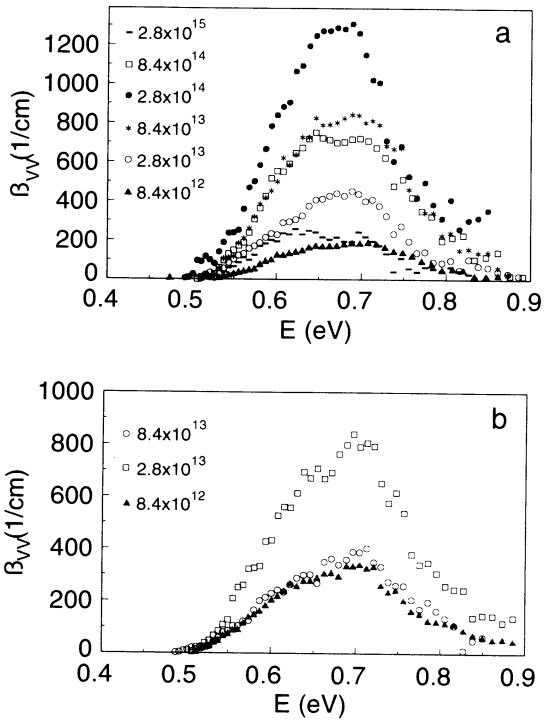

FIG. 3. Dose dependence of the divacancy absorption bands of SOS films. (a) Room-temperature implantation; (b) 80-K implantation.

The spectra show a progressive increase of the absorption with dose all over the investigated spectral region, due to the progressive accumulation of damage, as long as the implanted layer consisted of damaged crystalline material. When, with further dose increase, amorphous material also started forming in the layer, a decrease of the absorption in the spectra lower-energy region ($<\sim 1$ eV) occurs [8.4×10^{14} and 2.8×10^{15} cm^{-2} at 300 K in Fig. 1(b)], in agreement with earlier results obtained in bulk ion-implanted Si and GaAs.[21] The progressive growth and subsequent quenching of the absorption band at 0.69 eV (1.8 μm) due to the divacancy in its single positively, neutral, and single negatively charged states, is also evident. It should be pointed out that neither of the bands at 0.37 eV (3.3 μm) and 0.32 eV (3.9 μm) due, respectively, to the divacancy in its doubly negative and singly positive charged states, would be detectable as they would require the Fermi energy E_F to be positioned above ($E_C-0.4$) eV and below ($E_V+0.21$) eV respectively[12] (E_C and E_V are, respectively, the bottom of the conduction band and the top of the valence band). This is incompatible with our use of intrinsic material. According to a previously adopted procedure,[12,14] we have calculated the absorption due to the divacancy band alone (β_{VV}) by subtracting from the absorption spectra the contribution due to the background, determined by fitting the data away from the band. The results are shown in Figs. 3(a) and 3(b) for 300- and 80-K implantation, respectively. No divacancy absorption could be detected for the samples with the largest degree of damage, i.e., 80-K implantation with 2.8×10^{14} and 8.4×10^{14} cm^{-2}, where the implanted layer consisted mainly of amorphous material. From β_{VV} we have calculated the concentration of divacancies according to the relation, suggested in Ref. 13, N_{VV} (cm^{-3})$=7.7\times10^{16}\,\beta_{VV\,\max}$ ($\beta_{VV\,\max}$ is the maximum value of β_{VV} in the band) and the average number of divacancies produced per ion $R_{VV}=N_{VV}/l\Phi$, where Φ is the ion dose and l is the implanted layer thickness. Figure 4 reports the dose dependence of such quantities. N_{VV} initially increases, reaches a maximum value of $\sim10^{20}$ cm^{-3} at a dose of 2×10^{14} cm^{-2}, and then gradually becomes quenched for doses exceeding such a value. R_{VV}, on the other hand, initially shows a slight decrease which then becomes substantial for doses exceeding 2×10^{14} cm^{-2}. A similar result concerning N_{VV} had previously been obtained in bulk implanted Si where the maximum attained value was $\sim7\times10^{19}$ cm^{-3}.[14] Considering an average value of 1.5 ± 0.5 keV for the divacancy production energy,[14] this corresponds to an average energy deposited per unit volume of $\sim10^{20}$ keV/cm^3, an order of magnitude smaller than the average value required to induce complete amorphization in the implanted layer.

The mechanism which has been suggested as responsible for the decrease of the detected divacancies is self-quenching due to interaction amongst divacancies or interaction with other defects which anneal in parallel with the divacancies.[14] In fact, when a sample which had been implanted with a dose value such as to induce quenching

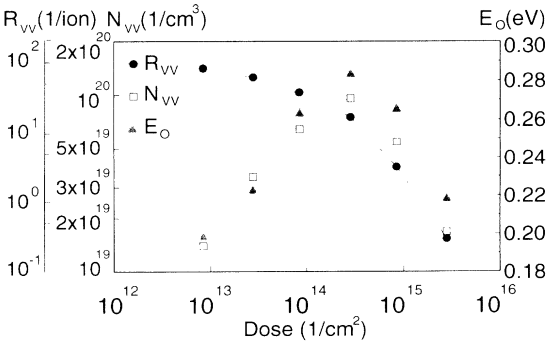

FIG. 4. Dose dependence of the average number of divacancies produced per ion (R_{VV}), divacancy concentration (N_{VV}), and band-edge inverse logarithmic slope (E_0) for room-temperature-implanted SOS films.

of β_{VV} was annealed at temperatures which eliminate divacancies (200–230 °C) and was then implanted with lower doses, the divacancy absorption and production rate which were obtained were similar to the ones obtained when implanting virgin crystalline material. Regarding the origin of the quenching process it has been suggested that, once a critical concentration of defects is exceeded, interaction of the divacancies with other divacancies and/or with other defects would induce, with respect to isolated divacancies, changes in their wave functions and energy levels or give rise to new complexes altogether, thus changing their optical as well as EPR response.[23] This is likely to occur for doses such that overlapping of the damage regions from the different ions becomes substantial, due to the considerable reduction induced in the average distance between the divacancies, and would cause the production rate of divacancies to become nonlinear with respect to the implantation dose. A considerable reduction in the average number of divacancies produced per ion would then be expected, as we report in Fig. 4 for doses exceeding the one corresponding to the maximum divacancy concentration.

Quenching of divacancies as detected by EPR has also been reported for concentration exceeding only 10^{19} cm^{-3}.[23] A word of caution should, however, be spent when EPR detection is involved. In fact the reduction in the observed concentration may be caused by a change in the charge state of the divacancy which would turn diamagnetic and thus become nondetectable by EPR. Accumulation of irradiation damage in Si is known to shift the Fermi energy progressively toward midgap,[24] and could well cause a change of the divacancy charge state from singly negative or singly positive to neutral. A reduction of the detected N_{VV} value could not, on the other hand, be attributed to the P doping of the Si used in Ref. 23 since P in Si is known to enhance the divacancy production by trapping the interstitial Si.[25] Thus, in this respect, divacancy detection through its 0.69-eV absorption band is of greater flexibility with respect to EPR, since it remains unaffected when the Fermi energy position ranges between $(E_C - 0.4)$ eV and E_V.[12]

In Fig. 4 we also report the dose dependence of the inverse-logarithmic slope E_0, which characterizes the exponential dependence of the absorption in the band-edge region ($\beta = \beta_0 \exp[E/E_0]$), where the absorption depends on the distribution of band-tail states. The E_0 values have been obtained by fitting the absorption data with such an exponential dependence in the band-edge regions of the spectra, as shown in Figs. 5(a) and 5(b). The dose dependence of E_0 closely correlates with the one of N_{VV}, which suggests that the electronic states associated with the divacancies strongly affect the population of band-tail states. This is consistent with the suggestion in Ref. 12 that the divacancy-associated states, from which the optical transitions originate, lie in the valence-band tail.

In Fig. 6 we show that the β_0 values we have obtained from the fit correlate very closely with the corresponding E_0 values. This should not be unexpected, since it has been shown that, when assuming nonconservation of momentum in the optical transitions and contribution to the optical absorption due to a single band-tail region, β_0 is proportional to E_0.[26] The first assumption should be justified for disordered semiconductors and the second one can be considered valid bearing in mind that in disordered Si (a-Si:H) it has been found that the conduction-band tail region is considerably steeper than the valence-band one.[27] Nonetheless, in spite of the strong correlation between such parameters, no unambiguous linear dependence between them can be obtained, as shown in the inset of Fig. 6, where we have also included the data relative to the 80-K, 8.4×10^{14}-cm^{-2} implantation which led to the formation of a uniform amorphous layer.

In Fig. 7 we report $(\beta E)^{1/2}$ vs E in order to probe the

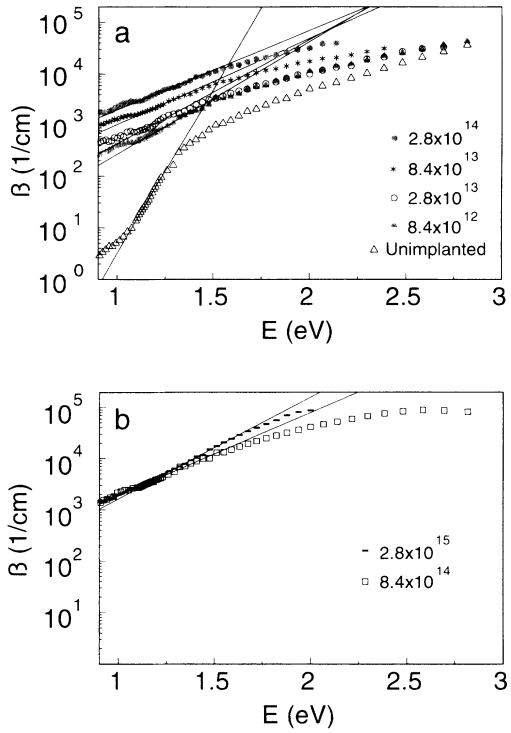

FIG. 5. (a), (b) Exponential fits in the band-edge regions of spectra of Figs. 1(a) and 1(b).

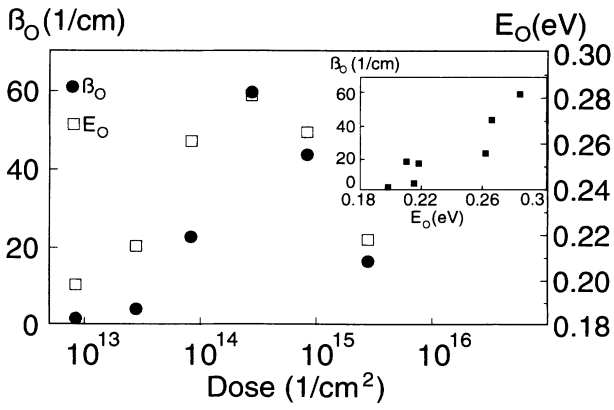

FIG. 6. Dose dependence of β_0 (see text) and E_0 for room-temperature-implanted SOS films. The mutual dependence of the parameters is shown in the inset.

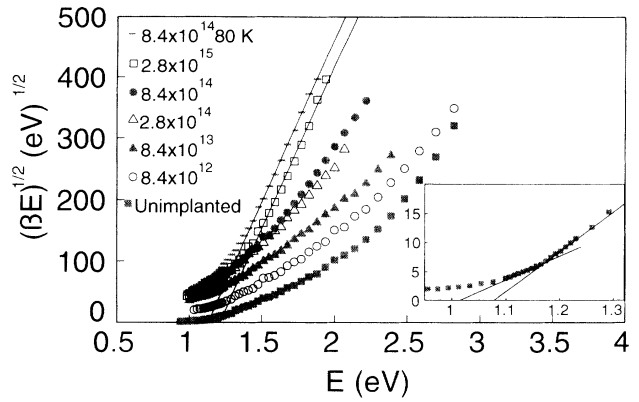

FIG. 7. Dose dependence of $(\beta E)^{1/2}$ vs E plots for implanted SOS films. The crystalline-material spectrum is shown in the inset.

effect of the implantation conditions on the value of the optical gap E_G, and on the dependence of the absorption coefficient on E_G near the band-edge region. For unimplanted crystalline Si, near the band-edge region, the absorption coefficient is given by

$$\beta E n_0 = \frac{(E-E_G-E_{\rm ph})^2}{1-\exp(-E_{\rm ph}/kT)} + \frac{(E-E_G+E_{\rm ph})^2}{\exp(E_{\rm ph}/kT)-1} ,$$

which reflects the phonon-assisted nature of the transitions,[28] where n_0 is the refractive index, $E_{\rm ph}$ is the phonon energy, and T is the temperature. For low enough values of the absorption, where direct transitions are not involved, the $(\beta E)^{1/2}$ vs E plot should yield a dual linear dependence as shown in the inset of Fig. 7. The linear fits through the two linear dependent regions yield intercepts on the abscissa whose arithmetic mean provides the value of E_G.[28] The value we obtain, 1.04±0.1 eV, is very close to the one obtained at 300 K, 1.08 eV, reported in Ref. 29. For amorphous material, on the other hand, for absorption values of the order of 10^4 cm^{-1}, the energy dependence of β is given by the Tauc formula $\beta E = K(E-E_G)^2$,[30] where K is a constant. A $(\beta E)^{1/2}$ vs E plot should then yield a linear dependence whose intercept on the abscissa provides E_G. This is what we obtain for the fully amorphized layer for which $E_G = 1.15$ eV. This value is larger than the one for the crystalline material but smaller than the ones obtained for other kinds of a-Si such as the ones obtained by room-temperature sputtering (1.26 eV)[31] and in a-Si:H (1.5–1.6 eV).[30] In Fig. 7, a good linear fit with the same angular coefficient as in the previous case is also obtained for the sample implanted at 300 K with a dose of 2.8×10^{15} cm^{-2} which contains amorphous material with residual damaged crystalline material. No specific dependence of β on E_G can be identified for the samples implanted with lower doses. The general trend is that, as expected, for increasing implantation dose the behavior shifts progressively from that of crystalline material toward that of amorphous material.

B. Annealing of damaged crystalline material

Figure 8 shows the spectra relative to the sample implanted at 300 K with a dose of 2.8×10^{14} cm^{-2}, which had originally shown the largest subgap absorption associated with divacancies and other defects, following isochronal annealings subsequently carried out for 15 min at increasing temperatures. The annealing temperature was increased in steps of 40 K between 393 and 433 K, 30 K between 433 and 463 K, 20 K between 463 and 523 K, and 50–70 K between 523 and 803 K. For the sake of clarity in the graphical representation we only report spectra relative to some of the intermediate annealing stages. Nevertheless, it is clear from the reported spectra that the absorption decreases all over the investigated spectral region with increasing annealing temperature. However, while an annealing at 803 K is sufficient to recover the absorption typical of the unimplanted material in the region above the band edge, this does not occur in the subgap region where the absorption is also affected by extended defects, like dislocations, which require much larger temperatures (1300–1400 K) to anneal out completely.

In the subgap region it can be observed that the band edge progressively sharpens with increasing annealing temperature, that the divacancy band is no longer detectable for annealing temperature larger than 483 K, and that an absorption band, typical of some intrinsic secondary defect, appears at 0.51 eV ($\sim$2.45 μm) for annealing temperatures exceeding 463 K and could no longer be detected following annealing at 803 K. These last three aspects are shown in greater detail in Figs. 9, 10, and 11, respectively. In particular, Fig. 10 shows that there is a strong correlation between the annealing behavior of the relative divacancy concentration and the band-edge inverse-logarithmic slope values, once more confirming that the divacancies strongly affect the population of band-tail states. Once the divacancies anneal out, the E_0 value remains constant around 0.14 eV up to the maximum annealing temperature reached in this work. This value is still considerably larger than the one we had obtained for unimplanted material (0.07 eV) in the plot shown in Fig. 5(a), and is probably associated with residual point defects, point-defect complexes, and strain induced by extended defects which survive up to much

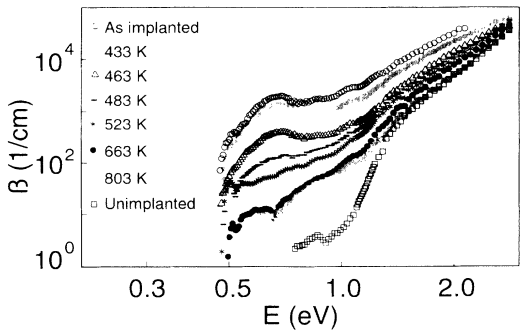

FIG. 8. Annealing-temperature dependence of the absorption spectra of a SOS film implanted at room temperature with a dose of 2.8×10^{14} cm^{-2}.

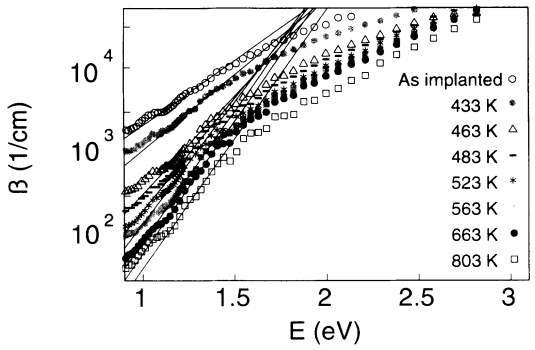

FIG. 9. Exponential fits in the band-edge regions of the spectra of Fig. 8.

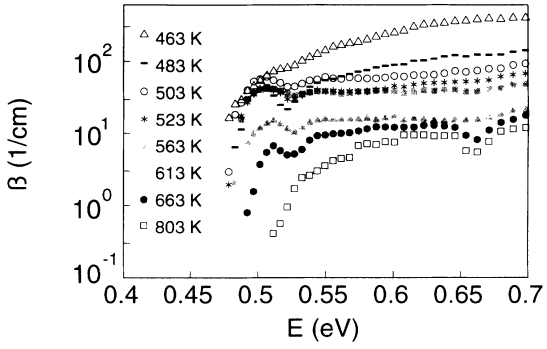

FIG. 11. Low-energy region of the spectra of the annealing dependence of the absorption spectra of the SOS film implanted at room temperature with a dose of 2.8×10^{14} cm^{-2}.

higher temperatures. It is interesting to note that such a value is similar to the one (0.13 eV) we obtain in implanted a-Si relaxed following an annealing for 2 h at 793 K, as shown later on in Fig. 16.

The annealing behavior of the 0.51-eV absorption band is shown in Fig. 11. From the spectra, the absorption due to the band alone is obtained by subtracting the background absorption as previously described, and the band peak absorption β_b is reported in Fig. 12 as a function of the annealing temperature. In an effort to find out the origin of such an absorption band, we have sought, amongst the known intrinsic secondary defects, for one whose annealing behavior resembled most of the one of our band. In Fig. 12 we have reported the comparison between the annealing behavior of the N center,[32] later identified as a five-vacancy complex,[10] and the one of our band. A close correlation between the two behaviors is evident, though certainly not conclusive. A more direct investigation is required to further clarify this point, involving parallel EPR and absorption measurements performed on the same sample after each annealing step.

We would finally like to point out in the spectra of Fig. 8 what appears to be a further broadband structure between 0.67 and 0.49 eV, which appears following annealing at 663 K. This structure will not be the subject of any further investigation in this work. It should just perhaps be mentioned that once more a similar structure appears in relaxed a-Si in Fig. 13 below.

ANNEALING OF AMORPHOUS MATERIAL

The study of the annealing on amorphous material, leading to the structural relaxation of ion-implanted a-Si, was performed on the sample implanted with a dose of 8.4×10^{14} cm^{-2} at 80 K, which, as stated earlier on, consisted of a uniform layer of amorphous material. Figure 13 shows the spectra relative to the as-implanted sample and to the sample after having undergone 15-min isochronal heat treatments, subsequently carried out at increasing temperatures, up to a maximum value of 793 K. Also shown is the spectrum relative to an additional annealing at 793 K for 1 h. Annealing for a total of 2 h at 793 K did not produce any further changes in the spectrum, which is therefore not reported. We note that, with the progressive increase in heat treatment, the absorption values decrease all over the investigated spectral region, while the absorption edge progressively shifts to larger energies and sharpens, as shown in greater detail in Figs. 14 and 15, where the changes in the band-edge slopes and in the Tauc plots are reported, respectively. The structural relaxation phenomenon thus leads to a continuous increase in the optical gap of the material and to a decrease in the inverse-logarithmic slope value. The evolutions of the two parameters vs temperature and time are reported in Fig. 16, which shows that the 1-h annealing at 793 K leads to a saturation of their values.

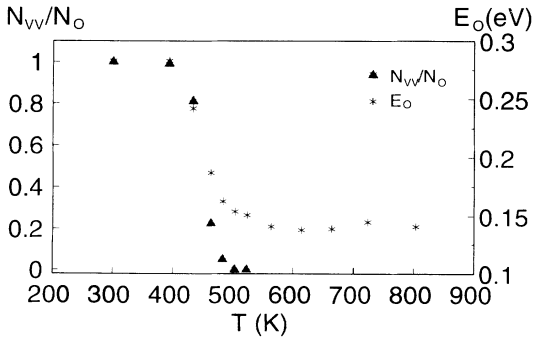

FIG. 10. Annealing-temperature dependence of relative N_{VV} values and of E_0 for the SOS film implanted at room temperature with a dose of 2.8×10^{14} cm^{-2}.

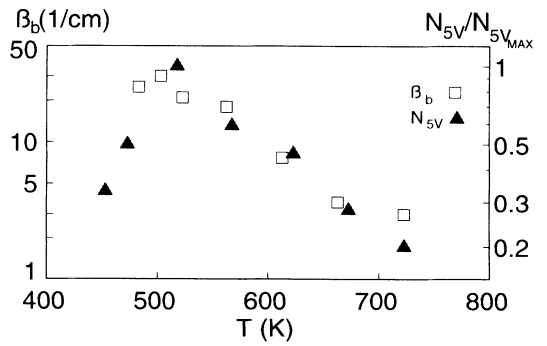

FIG. 12. Annealing-temperature dependence of the 0.51-eV band peak absorption (see text) and of the relative concentration of five-vacancy centers.

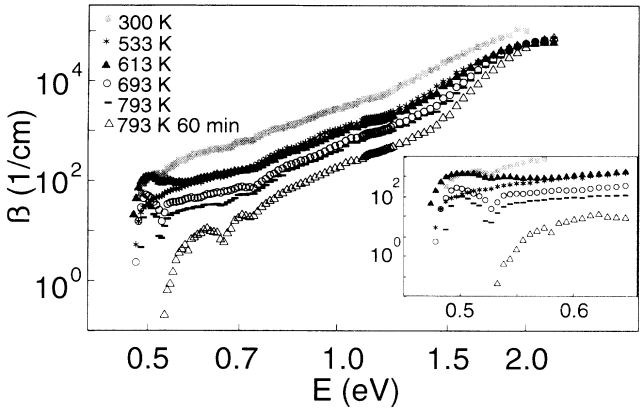

FIG. 13. Annealing temperature and duration dependence of the absorption spectra of an amorphous ion-implanted SOS film. Details of the low-energy region are shown in the inset.

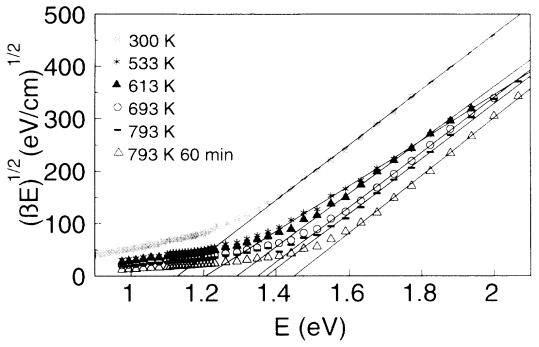

FIG. 15. Tauc plots (see text) of the spectra of Fig. 13.

The progressive sharpening of the band edge which is observed with increasing heat treatments is to be ascribed to the progressive reduction of strain in the material, which is known to affect the exponential absorption edge in semiconductors.[19] A reduction in strain, during the structural relaxation process in ion-implanted *a*-Si, has in fact been detected by Raman spectroscopy measurements,[6] and has also been related to the relaxation enthalpy detected by calorimetric measurements.[6] The progressive increase in E_G is also associated with occurring strain reduction as reported for structural-disorder-associated results in *a*-Si:H,[19] where it has been observed that a reduction in thermally or structurally induced disorder in the material also leads to an increase of E_G and a decrease of E_0. In particular, the authors in Ref. 19 describe both E_0 and E_G in terms of the mean square of the thermal- and disorder-induced displacement of the atoms from their equilibrium positions, and they eventually obtain a linear dependence between the two parameters supported by their experimental data and governed by the equation

$$E_G(T,X)=E_G(0,0)-\langle U^2\rangle_0 D\left[\frac{E_0(T,X)}{E_0(0,0)}-1\right],$$

where T is the temperature, X is a parameter describing structural disorder, $\langle U^2\rangle_0$ is the mean square of the zero-point uncertainty in the atomic position, and D is a second-order deformation potential. A linear fit to their E_G vs E_0 data yielded a slope of ~ 6.2 and, by using a value 0.08 Å for $\langle U^2\rangle_0^{1/2}$ and of 17 meV for $E_0(0,0)$,[19] the authors finally obtain $D=16$ eV/Å^2,[33] a value of the same order of magnitude as similar deformation potentials obtained in crystalline Ge (4–5 eV/Å^2).[34] This should confirm the validity of their approach. Finally, a value of 2.0 eV was obtained for $E_G(0,0)$ which should represent the upper limit for the band gap of the *a*-SiH$_x$ family of materials.

In Fig. 17 we report the E_G vs E_0 plot we obtain in the case of ion-implanted *a*-Si. The results clearly indicate a linear dependence between the parameters even in the case of implanted *a*-Si. The value of the slope of the linear-fit curve, 4.5, yields $D=13$ eV/Å^2, which is close to the value reported for *a*-Si:H. Even the value we obtain for $E_G(0,0)$, 1.9 eV, is consistent with the *a*-Si:H value. The strain-dependence behavior of both E_0 and E_G that we find in implanted *a*-Si is therefore in close agreement with the results reported for *a*-Si:H. In fact, the results concerning E_G we obtain are also similar to the ones reported during structural relaxation of *a*-Si films obtained by vacuum evaporation on a substrate at room temperature and then annealed for 2 h at 773 K.[31] Upon annealing, E_G changed from 1.26 to about 1.5 eV, a value which is very close to the one we obtain for the fully relaxed implanted *a*-Si (1.46 eV). The similarity in the

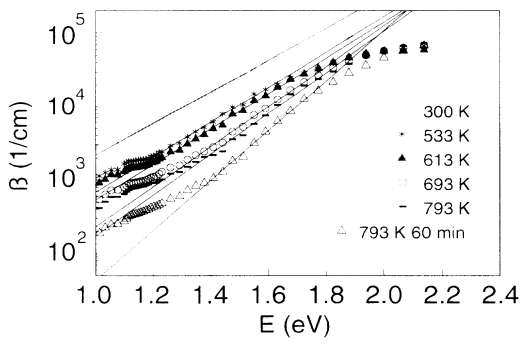

FIG. 14. Exponential fits in the band-edge regions of the spectra of Fig. 13.

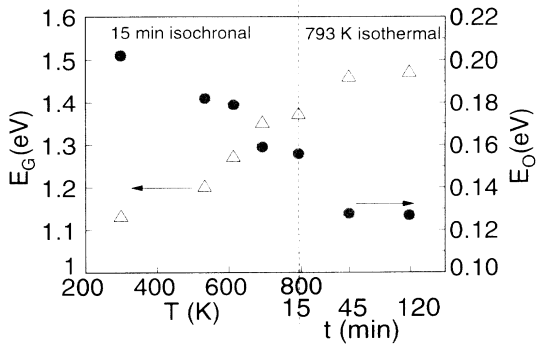

FIG. 16. Optical band gap E_G and E_0 as a function of the annealing conditions for an amorphous ion-implanted SOS film.

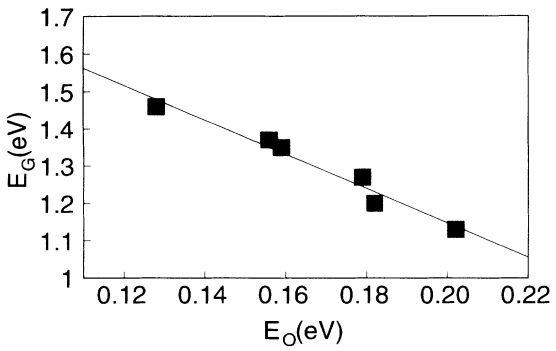

FIG. 17. E_G vs E_0 plot for the annealed amorphous ion-implanted SOS film.

strain-associated behaviors of E_G during the structural relaxation of a-Si films obtained by implantation and by evaporation is consistent with the similarity which is also observed in the results of calorimetric measurements performed during the relaxation of such films,[6] bearing in mind that, as stated earlier on, the calorimetric results have also been related to the strain reduction in the films. The results we have obtained at and above the band-edge region of ion-implanted a-Si thus confirm the occurrence of strain reduction during the structural relaxation process.

Regarding the subgap region of the spectra, as mentioned earlier on, the absorption in such a region depends on the defects present in the material. In a-Si:H the excess subgap absorption with respect to the exponential band tail, β_{ex}, has enabled the determination of the absolute concentration of dangling bonds over a range of three orders of magnitude.[20] According to an optical sum rule, such a concentration is proportional to the integral of β_{ex} over the subgap energy region and $\beta_{ex}=\beta-\beta_0\exp(E/E_0)$. We have performed such integrals for the as-implanted sample and for the sample which had undergone maximum relaxation using the β_0 and E_0 obtained earlier through a fit of the absorption data in the respective band-edge regions. We have found a reduction of nearly a factor of 5 in the integral calculated for the sample which had undergone maximum relaxation with respect to the one calculated for the as-implanted sample. The reduction is therefore greater than the factor 2 reported for the decrease in concentration of dangling bonds alone in relaxed ion-implanted a-Si as determined by electron paramagnetic resonance,[35] and almost the same as the one reported for the reduction of point-defect concentration in relaxed material ($\sim$ factor 5) as determined by metal diffusion and solubility measurements.[6,18] The results we have obtained, therefore, point in the same direction as earlier suggestions, and that is that the structural relaxation process in ion-implanted a-Si is accompanied by point-defect annihilation. In this respect it is also interesting to point out that, even in these samples, an absorption band appears in the subgap absorption spectra near 0.51 eV (see inset of Fig. 13) at the annealing temperature 0f 613 K, gradually decreases for higher temperatures, and is no longer detectable when the sample becomes fully relaxed. Such an evolution should indicate the formation of some secondary defect complexes during the intermediate stages of the annealing, as also observed in damaged crystalline material, and should thus be evidence of defect mutual interaction. The absorption-band spectral position and annealing behaviors are very similar to those found in the case of the annealing of damaged crystalline material, where we have tentatively associated it with the five-vacancy complex. Although primary point defects like vacancies and vacancy-impurity complexes have been detected in ion-implanted amorphous material,[7] EPR spectra of the five-vacancy complex could not be detected following annealing of an implanted layer which initially appeared to consist solely of amorphous material (random RBS spectrum as in our amorphous sample) but could be detected in a sample initially consisting of amorphous and damaged crystalline material.[36] The possibilities are then that either the band we have observed does not originate from the five-vacancy complex or the amorphous layer we have investigated originally contained even some residual clusters of damaged crystalline material. Perhaps some other explanations or interpretations are possible, but further work is certainly required to clarify this issue.

CONCLUSIONS

We have presented a detailed study of the implantation-induced effects in Si on sapphire films through optical-absorption measurements carried out form energies above the band gap down to energies far into the subgap region of the material. The changes induced in the optical band gap, band-edge region, and subgap features of the spectra have been carefully analyzed as a function of the implantation and subsequent annealing conditions.

In damaged crystalline material, the various stages of formation and quenching of the divacancies were monitored through their 0.69-eV (1.8-μm) absorption band. Correlation of the behaviors of such bands with that of the band-edge slope as a function of implantation dose and annealing cycles has shown that divacancies strongly affect the population of band-tail states. Moreover, the annealing studies revealed the progressive quenching of the divacancy band followed by the appearance of another absorption band, peaked at about 2.45 μm and characteristic of some secondary intrinsic defect, whose annealing behavior is very similar to the one observed for the EPR spectrum of the five-vacancy complex.

Studies carried out on an amorphous ion-implanted film as a function of annealing conditions allowed the investigation of the structural relaxation process in ion-implanted a-Si. It has been observed that, in agreement with earlier observations, the relaxation process is associated with strain reduction in the material which leads to a progressive sharpening of the band edge and an increase of the optical gap of the material until a value of $\sim$1.5 eV is reached, consistently with values obtained in relaxed evaporated a-Si and in hydrogenated a-Si. Moreover, changes occurring upon relaxation of the material in the subgap region of the spectra are consistent with

earlier evidence that the relaxation process is accompanied by evolution and annihilation of point defects and point-defect complexes. Finally, some common features, such as band-edge inverse-logarithmic slope values and subgap features, are found in annealed implanted crystalline and *a*-Si.

ACKNOWLEDGMENTS

One of the authors (K.N.M.) acknowledges financial support from I.C.T.P. Trieste. The research was partially supported by the Italian Ministry of Scientific Research and National Research Council.

[1]H. Wong, N. W. Cheng, P. K. Chu, J. Liu, and J. W. Mayer, Appl. Phys. Lett. **52**, 1023 (1988).

[2]M. Tamura, T. Ando, and K. Onyu, Nucl. Instrum. Methods Phys. Res. Sect. B **59/60**, 572 (1991).

[3]W. X. Lu, Y. H. Qian, R. H. Tian, Z. L. Wang, R. J. Schreutelkamp, J. R. Liefting, and F. W. Saris, Appl. Phys. Lett. **55**, 1838 (1989).

[4]R. J. Schreutelkamp, J. S. Custer, J. R. Liefting, W. X. Lu, and F. W. Saris, Mater. Sci. Rep. **6**, 275 (1991).

[5]D. E. Polk, J. Non-Cryst. Solids **5**, 365 (1971).

[6]See, for example, S. Roorda, W. C. Sinke, J. M. Poate, D. C. Jacobson, S. Dierker, B. S. Dennis, D. J. Eaglesham, F. Spaepen, and F. Fuoss, Phys. Rev. B **44**, 3702 (1991).

[7]G. N. Van den Hoven, Z. N. Liang, and L. Niesen, Phys. Rev. Lett. **68**, 3714 (1992).

[8]G. D. Watkins and J. W. Corbett, Phys. Rev. **138**, A543 (1965).

[9]K. L. Brower, Radiat. Eff. **8**, 213 (1971).

[10]Y. H. Lee and J. W. Corbett, Phys. Rev. B **8**, 2810 (1973).

[11]Y. H. Lee, N. N. Gerasimenko, and J. W. Corbett, Phys. Rev. B **14**, 4506 (1976).

[12]L. J. Cheng, J. C. Corelli, J. W. Corbett, and G. D. Watkins, Phys. Rev. **152**, 761 (1966).

[13]L. J. Cheng and J. Lori, Phys. Rev. **171**, 856 (1968).

[14]H. J. Stein, F. L. Vook, D. K. Brice, J. A. Borders, and S. T. Picraux, Radiat. Eff. **6**, 19 ((1970).

[15]K. L. Brower, F. L. Vook, and J. A. Borders, Appl. Phys. Lett. **16**, 108 (1970).

[16]G. Müller and S. Kabiltzer, Philos. Mag. B **38**, 241 (1978).

[17]S. Coffa, F. Priolo, J. M. Poate, and S. H. Glarum, Nucl. Instrum. Methods Phys. Res. Sect. B **80/81**, 603 (1993).

[18]S. Coffa, J. M. Poate, D. C. Jacobson, W. Frank, and W. Gustin, Phys. Rev. B **45**, 8355 (1992).

[19]G. D. Cody, T. Tiedje, B. Abeles, and Y. Goldstein, Phys. Rev. Lett. **47**, 1480 (1981).

[20]N. Amer and J. D. Jackson, in *Semiconductors and Semimetals,* edited by J. I. Pankove (Academic, New York, 1984), Vol. 21B, p. 83.

[21]U. Zammit, F. Gasparrini, M. Marinelli, R. Pizzoferrato, A. Agostini, and F. Mercuri, J. Appl. Phys. **70**, 7060 (1991); U. Zammit, M. Marinelli, R. Pizzoferrato, and F. Mercuri, Phys. Rev. B **46**, 7515 (1992).

[22]D. Ritter and K. Weiser, Opt. Commun. **57**, 336 (1986).

[23]K. L. Brower and Wendland Beezhold, J. Appl. Phys. **43**, 3499 (1972).

[24]E. Sonder and L. C. Templeton, J. Appl. Phys. **34**, 3295 (1963).

[25]B. G. Svensson and J. L. Lindström, J. Appl. Phys. **72**, 5616 (1992).

[26]J. I. Pankove, Phys. Rev. **140**, A2029 (1965).

[27]T. Tiedje, J. M. Cebulka, D. L. Morel, and B. A. Abele, Phys. Rev. Lett. **46**, 1425 (1981).

[28]N. F. Mott and E. A. Davies, *Electronic Processes in Noncrystalline Materials* (Clarendon, Oxford, 1979), p. 274.

[29]G. G. MacFarlane and V. Roberts, Phys. Rev. **98**, 1865 (1955).

[30]N. F. Mott and E. A. Davies, *Electronic Processes in Noncrystalline Materials* (Ref. 28), p. 387.

[31]A. Lewis, Phys. Rev. Lett. **29**, 1555 (1972).

[32]W. Jung and G. S. Newell, Phys. Rev. **132**, 648 (1963).

[33]The authors actually quote a value of ~ 30 eV/Å^2. However, going through their calculations we obtain a value of 16 eV/Å^2.

[34]B. Allen and M. Cardona, Phys. Rev. B **23**, 1495 (1981).

[35]C. N. Waddell, W. G. Spitzer, J. E. Friedrickson, G. K. Hubler, and T. A. Kennedy, J. Appl. Phys. **55**, 4361 (1984).

[36]L. Sealy, R. C. Barklie, W. L. Brown, and D. C. Jacobson, Nucl. Instrum. Methods Phys. Res. Sect. B **80/81**, 528 (1993).